

Microwave-mediated heat transport in a quantum dot attached to leads

Feng Chi¹, Yonatan Dubi²

¹ College of Engineering, Bohai University, Jinzhou 121013, China

² Landa Laboratories, 3 Pekeris St., Rehovot 76702, Israel

E-mail: chifeng@semi.ac.cn

Abstract. The thermoelectric effect in a quantum dot (QD) attached to two leads in the presence of microwave fields is studied by using the Keldysh nonequilibrium Green function technique. When the microwave is applied only on the QD and in the linear-response regime, the main peaks in the thermoelectric figure of merit and the thermopower are found to decrease, with the emergence of a set of photon-induced peaks. Under this condition the microwave field can not generate heat current or electrical bias voltage. Surprisingly, when the microwave field is applied only to one (bright) lead and not to the other (dark) lead or the QD, heat flows mostly from the dark to the bright lead, almost irrespectively to the direction of the thermal gradient. We attribute this effect to microwave-induced opening of additional transport channels below the Fermi energy. The microwave field can change both the magnitude and the sign of the electrical bias voltage induced by the temperature gradient.

PACS numbers: 73.21.La, 72.15.Jf, 73.50.Pz, 73.23.Hk

1. Introduction

Owing to the possibility of high heat-voltage conversion efficiency, thermoelectric phenomenon in nanoscale solid-state materials has become an active research area in recent years[1,2]. In the linear response regime, i.e., the temperature gradient in the device ΔT approaches to zero, the thermoelectric efficiency is measured by the dimensionless thermoelectrical figure of merit ZT , and is usually smaller than one in bulk materials[3]. This hinders the wide usage of thermoelectric effect in commercial applications. The reason behind the small ZT in bulk materials is the Wiedemann-Franz law[4], which can be violated in nanoscale materials, for instance due to the Coulomb blockade effect[5]. In the nonlinear response regime, i.e., finite ΔT case, the thermoelectric energy conversion efficiency is characterized by the bias voltage ΔV generated by ΔT [6]. In both of linear and nonlinear cases, the thermoelectric efficiency in nanostructures may be much higher than that in bulk materials because of the reduced dimensionality[7-9], and more interestingly, depends on the quantized energy levels that can be modulated by gate voltages. Since the breakthroughs in experimental work[10-14], large figure of merit exceeding one or higher and large ΔV were frequently reported in superlattices, quantum wires, quantum dots, and carbon nanotubes, etc. Theoretically, impacts of Coulomb blockade[5-9,15-20], Kondo[21-24], and Fano[25,26] effects on the thermoelectric properties were extensively investigated. Applications such as nanoscale refrigeration[27], thermal rectifier[18,28,29], thermal transistors[6], and thermal memory and logic gates[30] were proposed.

The above-mentioned works mainly focused on the thermoelectric efficiency under time-independent fields. Very recently, heat transport with photons has also been studied. It was demonstrated that heat can be conducted by photon radiation at very low temperature when the phonons are frozen out[31]. Quantum circuits sandwiched between two reservoirs and threaded by electromagnetic fluctuations (photons) were proposed to operate as heat transistors or electron coolers[32,33]. In a double-quantum-well structure, it was shown that hotter electrons in one reservoir may be replaced by the cooler ones in the other reservoir with the help of photon by adjusting the wells' energy levels[34]. Electron heating in two-dimensional electron system has also been theoretically and experimentally investigated[35]. In addition, Lau *et al.* have calculated the properties of coherent radiative thermal conductance in photonic crystals[36]. Moreover, enhanced thermopower (Seebeck coefficient) induced by a time-dependent gate voltage was proposed in a device of a quantum dot (QD) coupled to two metal leads[37].

As a zero-dimensional system, QD is a promising thermoelectrical material and was intensively studied in many of the above mentioned works. Until now, photon-assisted heat transport in such a device has seldom been addressed, although it has been studied in the context of electron transport through QDs long time ago[38,39]. In this paper, we study the photon-mediated thermoelectric effect in a QD attached to two leads in both linear ($\Delta T \rightarrow 0$) and nonlinear (finite ΔT) regimes. Compared with previous studies on

quantum circuits[32,33], we deal with a relatively high temperature situation. Our main results show that when the microwave field is applied only on the QD, the magnitude of the figure of merit is suppressed because of the photon-induced sub-channels in the dot. When the microwave is applied only on one lead, large heat current and electric bias are generated. We find that the heat current generally flows from the dark lead into the bright one, except for the situation in which the dot level is around the electron-hole symmetry point. In the present paper, the contributions from phonons are neglected for the sake of simplicity.

2. Model and method

The present system can be described by the following Hamiltonian[39,40]:

$$\begin{aligned}
 H(t) = & \sum_{k,\sigma,\beta} \varepsilon_{k\beta}(t) c_{k\beta\sigma}^\dagger c_{k\beta\sigma} + \sum_{\sigma} \varepsilon_d(t) d_{\sigma}^\dagger d_{\sigma} + U d_{\uparrow}^\dagger d_{\uparrow} d_{\downarrow}^\dagger d_{\downarrow} \\
 & + \sum_{k,\sigma,\beta} (V_{\beta d} c_{k\beta\sigma}^\dagger d_{\sigma} + \text{H.c.}), \tag{1}
 \end{aligned}$$

where $c_{k\beta\sigma}^\dagger$ ($c_{k\beta\sigma}$) is the creation (annihilation) operator of the electrons with momentum k , spin σ and energy $\varepsilon_{k\beta}(t)$ in the β ($= L, R$) lead; d_{σ}^\dagger (d_{σ}) creates (annihilates) an electron with spin σ , energy $\varepsilon_d(t)$ in the QD. U denotes the intradot Coulomb interaction. The last term in Eq. (1) represents the dot-lead coupling with coupling strength $V_{\beta d}$. The time-varying energy spectra originate from the applied microwave fields and take the forms of $\varepsilon_{k\beta}(t) = \varepsilon_{k\beta} + \Delta_{\beta} \cos \omega t$ and $\varepsilon_d(t) = \varepsilon_d + \Delta_d \cos \omega t$, where $\varepsilon_{k\beta}$ and ε_d are the time-independent single electron energies without microwave field, and $\Delta_{\beta/d}$, ω are respectively the microwave strength and frequency applied on the leads or the dot[39,40].

Time-dependent electric and heat currents from lead β to the QD can be calculated from the evolution of the total number operator of the electrons in the lead (in unit of $\hbar = 1$)[39],

$$\begin{pmatrix} J_{\beta\sigma}(t) \\ Q_{\beta\sigma}(t) \end{pmatrix} = \frac{d}{dt} \left\langle \sum_k \begin{pmatrix} -e \\ \varepsilon_{k\beta}(t) - E_F(t) \end{pmatrix} c_{k\beta\sigma}^\dagger c_{k\beta\sigma} \right\rangle, \tag{2}$$

where $E_F(t) = e[\mu_L(t) - \mu_R(t)]$ is the Fermi level. The total electric and heat currents are $J(t) = \sum_{\sigma} [J_{L\sigma}(t) - J_{R\sigma}(t)]$ and $Q(t) = \sum_{\sigma} [Q_{L\sigma}(t) - Q_{R\sigma}(t)]$, respectively. In this paper we are interested in the time averaged electric and heat currents, which can be derived following the standard Keldysh Green function technique as[39]:

$$\begin{pmatrix} J \\ Q \end{pmatrix} = \frac{2}{\hbar} \frac{\Gamma_L \Gamma_R}{\Gamma_L + \Gamma_R} \sum_{\sigma} \int d\varepsilon \begin{pmatrix} -e \\ \varepsilon - E_F \end{pmatrix} \times [f_L(\varepsilon) \text{Im}\langle A_{L\sigma}(\varepsilon, t) \rangle - f_R(\varepsilon) \text{Im}\langle A_{R\sigma}(\varepsilon, t) \rangle], \tag{3}$$

where the line-width function $\Gamma_{L(R)} = 2\pi \sum_k V_{L(R)d} V_{L(R)d}^* \delta(\varepsilon - \varepsilon_k)$ is assumed to be independent of the energy under wide bandwidth approximation. $f_{\beta}(\varepsilon) = [1 + e^{(\varepsilon - \mu_{\beta})/k_B T_{\beta}}]^{-1}$ is the Fermi distribution function of lead β with chemical potential μ_{β} ,

temperature T_β and Boltzmann constant k_B . The quantity $A_{\beta\sigma}(\varepsilon, t)$ is defined through the Green function as

$$A_{\beta\sigma}(\varepsilon, t) = \int_{-\infty}^t dt_1 G_\sigma^r(t, t_1) \exp[-i\varepsilon(t_1 - t) - i \int_t^{t_1} \Delta_\beta(\tau) d\tau], \quad (4)$$

where $G_\sigma^r(t, t_1) = -i\theta(t - t') \langle \{d_\sigma(t), d_\sigma^\dagger(t')\} \rangle$ is the retarded Green function, which can be obtained by the equation of motion technique following the processes in Ref. [40]:

$$\begin{aligned} G_\sigma^r(t, t') = & -i\theta(t - t') \left\{ (1 - n_{\bar{\sigma}}) \exp\left(-i \int_{t'}^t \varepsilon_d(\tau) d\tau - \frac{\Gamma}{2}(1 - n_{\bar{\sigma}})(t - t')\right) \right. \\ & \left. + n_{\bar{\sigma}} \exp\left(-i \int_{t'}^t [\varepsilon_d(\tau) + U] d\tau - \frac{\Gamma}{2}n_{\bar{\sigma}}(t - t')\right) \right\}. \end{aligned} \quad (5)$$

It should be noted that the adopted decoupling approximation to higher-order many-particle Green functions is sufficient for electronic transport in the Coulomb blockade regime, but not for higher-order tunneling process such as the subtle Kondo effect, which is beyond the consideration of this paper. In the above equation, $\Gamma = \Gamma_L + \Gamma_R$. Substituting the expression of the retarded Green function into Eq. (4) and carrying out the integrations, $A_{\beta\sigma}(\varepsilon, t)$ becomes

$$\begin{aligned} A_{\beta\sigma}(\varepsilon, t) = & \sum_{k, k'} J_k \left(\frac{\Delta_d - \Delta_\beta}{\omega} \right) J_{k'} \left(\frac{\Delta_\beta - \Delta_d}{\omega} \right) e^{i(k+k')\omega t} \\ & \times \left\{ \frac{1 - n_{\bar{\sigma}}}{\varepsilon - \varepsilon_d - k'\omega + i\Gamma(1 - n_{\bar{\sigma}})/2} + \frac{n_{\bar{\sigma}}}{\varepsilon - \varepsilon_d - U - k'\omega + i\Gamma n_{\bar{\sigma}}/2} \right\}, \end{aligned} \quad (6)$$

where J_k are Bessel functions of the first kind. The occupation number $n_{\bar{\sigma}}$ in the above equations needs to be calculated self-consistently from the equation

$$n_{\bar{\sigma}} = \langle \text{Im} G_{\bar{\sigma}}^<(t, t) \rangle = \int \frac{d\varepsilon}{2\pi} \sum_{\beta} f_{\beta}(\varepsilon) \Gamma_{\beta} \langle |A_{\beta\bar{\sigma}}(\varepsilon, t)|^2 \rangle, \quad (7)$$

where $G_{\bar{\sigma}}^<(t, t)$ is the lesser Green function that can be calculated by the Keldysh equation with the help of the retarded Green function. Once $A_{\beta\sigma}(\varepsilon, t)$ is determined, the currents can be calculated from its time-averaged form:

$$\begin{aligned} \langle A_{\beta\sigma}(\varepsilon, t) \rangle = & \sum_k J_k^2 \left(\frac{\Delta_d - \Delta_\beta}{\omega} \right) \\ & \times \left[\frac{1 - n_{\bar{\sigma}}}{\varepsilon - \varepsilon_d - k\omega + i\Gamma(1 - n_{\bar{\sigma}})/2} + \frac{n_{\bar{\sigma}}}{\varepsilon - \varepsilon_d - U - k\omega + i\Gamma n_{\bar{\sigma}}/2} \right]. \end{aligned} \quad (8)$$

3. Results

Let us start by considering the case where the microwave field is applied only on the dot, i.e. $\Delta_L = \Delta_R = 0$ and $\Delta_d \neq 0$. In the following numerical calculations, we set $\hbar = 1$ and choose the microwave field frequency $\omega = 1$ as the energy unit. In the linear

response regime ($T_L = T_R = T$) the electric current in Eq. (3) can be written in the following compact form:

$$J = -\frac{2e}{h} \int d\varepsilon [f_L(\varepsilon) - f_R(\varepsilon)] T(\varepsilon), \quad (9)$$

where the transmission coefficient $T(\varepsilon)$ is

$$T(\varepsilon) = \frac{\Gamma_L \Gamma_R}{\Gamma_L + \Gamma_R} \sum_{k,\sigma} J_k^2 \left(\frac{\Delta_d}{\omega} \right) \times \left[\frac{1 - n_{\bar{\sigma}}}{\varepsilon - \varepsilon_d - k\omega + i\Gamma(1 - n_{\bar{\sigma}})/2} + \frac{n_{\bar{\sigma}}}{\varepsilon - \varepsilon_d - U - k\omega + i\Gamma n_{\bar{\sigma}}/2} \right]. \quad (10)$$

We subsequently introduce the integrals $I_n(T)$ with $n = 0, 1, 2$, $I_n(T) = -(2/h) \int \varepsilon^n (\partial f / \partial \varepsilon) T(\varepsilon) d\varepsilon$. The linear conductance G , thermopower S , and the thermal conductance κ can be expressed as

$$\begin{aligned} G &= e^2 I_0(T), \\ S &= -I_1(T) / [eT I_0(T)], \\ \kappa &= (1/T) [I_2(T) - I_1^2(T) / I_0(T)]. \end{aligned} \quad (11)$$

Neglecting the thermal conductance from the phonons as is assumed here, the figure of merit ZT is given by

$$ZT = GS^2T / \kappa. \quad (12)$$

Figure 1 shows the behaviors of G , κ , S , and ZT versus dot level ε_d for different microwave field strength Δ_d . For $\Delta_d = 0$, the linear conductance G in Fig. 1(a) shows two peaks respectively positioned at $\varepsilon_d = 0$ and $-U$, exhibiting the typical Coulomb blockade effect. As for the thermal conductance κ in Fig. 1(b), two smooth shoulders emerge around the two main peaks. When the microwave field is applied on the dot, photon-induced peaks emerge in G at $0 \pm k\omega$ and $-U \pm k\omega$, where k is an integer. Meanwhile, the height of the main peaks is reduced. The reason is that the microwave field excites more conduction channels in the dot, and then the transmission probabilities through the channels of $\varepsilon_d = 0$ and $-U$ are shared and suppressed. As for the thermal conductance κ , the height of the main peaks first increases and then decreases with the increase of the microwave field strength. This is because κ is determined by both the transmission probability and the heat transferred by each electron. Contrary to the situation in G , each main peak in κ around $\varepsilon_d = 0$ or $-U$ is contributed from more than one conduction channels, which can be seen by comparing Fig. 1(b) with 1(a). Thus, their height may be enhanced even if the average tunnelling probability of each channel decreases. Here the function of the microwave field is analogous to the changing of temperature in the leads[18-20], which adjusts the numbers of the electron and hole around the Fermi level to participate in transport. With increasing temperature T , the average tunneling probability will be monotonically suppressed but the heat carried by each electron increases. As a result, the height of the peaks in κ will exhibit a nonmonotonic dependence on T [19, 20], which is different from the behavior of the

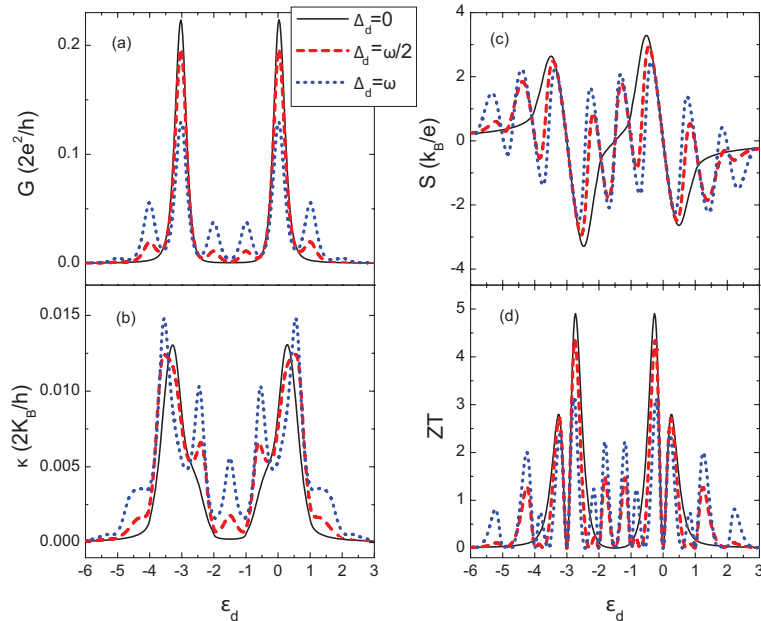


Figure 1. (Color online) Electrical conductance G , thermal conductance κ , thermal power S , and figure of merit ZT as functions of dot level ε_d for different microwave field strength Δ_d with $\Delta_L = \Delta_R = 0$. Other parameters are $U = 3\omega$, $k_B T = 0.1\omega$, and $\Gamma_L = \Gamma_R = 0.05\omega$. The presence of a microwave field is seen to decrease the strength of the main peaks of the thermoelectric figure of merit, and a set of additional peaks in multiples of the microwave frequency emerges.

peaks in G . We also observe that a peak in the thermal conductance develops at the electron-hole symmetry point $-U/2$ due to the application of the microwave field. This may be attributed to the photon-induced conduction channels around this point, which can be seen from Fig. 1(a).

The thermopower S in Fig. 1(c) has three zero points individually at $\varepsilon_d = -U$, $-U/2$ (electron-hole symmetry point), and 0. The magnitude of S oscillates between these three points with positive and negative values, which can be understood as follows[19,20]: In the presence of temperature difference that induces the thermoelectric phenomenon, there are more electrons above the chemical potential $\mu = 0$ in the hotter lead, and at the same time more holes in the cooler lead below μ . When the dot energy levels ε_d or $\varepsilon_d + U$ is above μ , more electrons will transport from the left lead of higher temperature to the right lead of lower temperature than the holes tunnelling from the opposite direction, inducing a positive voltage drop ΔV and consequently a negative thermopower $S = -\Delta V/\Delta T$ (S is negative in the figure as in unit of k_B/e). When the energy levels are aligned to the chemical potential or the electron-hole symmetry point, the voltage drop induced by the electrons are cancelled by that of the holes. Thus the thermopower is zero. When ε_d or $\varepsilon_d + U$ is below the chemical potential, more electrons tunnel from right to left and S changes sign. The above explanation also holds true when the microwave field is applied. Now a set of sub-channels are opened by the photons, inducing more zero points in S . Consequently, the applied microwave field can change

the sign of S , which may be used to detect the properties of the microwave field. Fig. 1(d) shows that the magnitude of the main peaks in ZT is reduced by the microwave field with the emergence of a set of shoulder peaks. This is because of the combined effect of reduced linear conductance and enhanced thermal conductance. Although the original peaks height is lowered by the microwave field, there are several new peaks that can reach quite large value, and may be useful for energy conversion.

Figure 2 shows the temperature-dependence of ZT for different microwave field strength Δ_d . To acquire a large ZT value, the dot level is fixed at -0.25ω , where the main peak in ZT is centered. It is shown that the ZT value first increases and then decreases after reaching a maximum value with the increase of the temperature, which is consistent with previous result [18-20]. The magnitude of ZT is determined by the combined behavior of G , κ , and S . Detailed dependence of these quantities on the temperature can be found in Refs. 19 and 20. For $k_B T \ll U$, the ZT value is considerably enhanced due to the Coulomb blockade effect, and optimal thermoelectric efficiency can be achieved in this region. With the increase of the temperature, the peaks in ZT is suppressed as the influence of Coulomb blockade effect on electron transport becomes less important. In the presence of the microwave field, the line-shape of ZT is reserved but with reduced strength. This is consistent with the above result. With the increase of the microwave field strength, the maximum ZT value shifts to lower temperature regime.

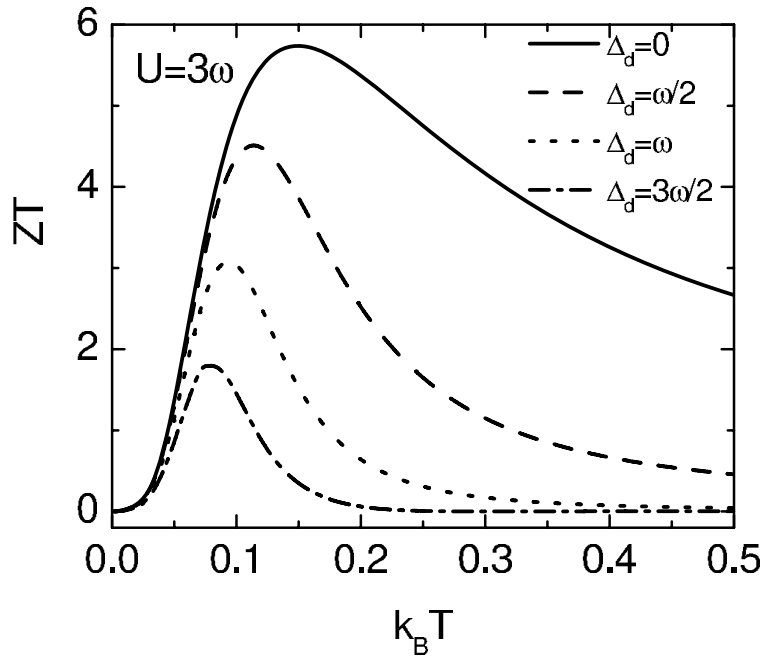


Figure 2. ZT as a function of $k_B T$ for different microwave field strength $\Delta_d = 0, \omega/2, \omega, 3\omega/2$ with $\Delta_L = \Delta_R = 0$. Other parameters are as in Fig. 1. The effect of microwave field applied only to the quantum dot is a string reduction of ZT .

When the microwave field is asymmetrically applied to the structure, heat current and bias voltage will be generated under the condition of zero electrical current (this

condition is easily met in thermopower experiments [1,2]). From Eqs. (3) and (8), now the heat current is mainly determined by the difference between the microwave field strength in the dot Δ_d and that in the leads $\Delta_{L/R}$. We thus consider the case of a field applied only on the leads. For comparison, we first present the results without any microwave in Fig. 3(a-b). It shows that the heat current always flows from the hotter lead to the cooler one under a thermal bias ΔT . It has a main resonance when the dot level is located on the electron-hole symmetry point, and two dips when ε_d and $\varepsilon_d + U$ are aligned to the chemical potential $\mu = 0$. The reason behind this is as follows: When ε_d and $\varepsilon_d + U$ are aligned to the chemical potential, the energy difference between the electrons from different leads, which are tunnelling in opposite directions through these levels, is relatively small, resulting in small heat current. But when the dot level is at the symmetry point $\varepsilon_d = -U/2$, electrons in the left lead tunnel to the right lead through the level of $\varepsilon_d + U = U/2$, which is above the chemical potential and have larger thermal energy. Meanwhile, equal number electrons tunnel from the right lead through the level of $-U/2$ to the left one with less thermal energy. In other words, holes tunnel from the left lead to the right lead through $-U/2$. The contributions from the electrons and holes to the heat current add constructively, giving rise a high peak. Other smaller resonances in Fig. 3(a) can be explained by similar reasons. The bias voltage ΔV in Fig. 3(b) has three zero points at energy levels of $\varepsilon_d = 0, -U$ and $-U/2$, because where equal numbers are flowing from opposite directions. Apart from these levels, it oscillates between negative and positive values. The reason is just the same as that of the thermopower in Fig. 1(c). If there is microwave field applied on the QD as shown in Fig. 3(c-d), the trends of the heat current and electrical bias voltage are preserved, except for the emergence of a set of smaller peaks. The heat current magnitude is enhanced because there are more carriers participating in transport through the photon-induced sub-channels.

Let us now consider the situation when the microwave field is applied only to the left lead. Fig. 4(a-b) shows the heat current and the induced electric voltage as functions of the dot level for various temperature differences with $\Delta_d = \Delta_R = 0$ and $\Delta_L = \omega$. Compared to the cases in Figs. 3(a-b) and 3(c-d), the magnitude of the heat current is remarkably enhanced as the dot levels ε_d and $\varepsilon_d + U$ are slightly higher and lower than zero. For positive thermal bias $k_B \Delta T > 0$, the heat current can flow from the right cooler (dark) lead to the left hotter (bright) lead except for ε_d is in the middle of the Coulomb blockade regime, which is shown in Fig. 4(a). For negative thermal bias $k_B \Delta T < 0$, the heat current always flow from the right hotter (dark) lead to the left cooler (bright) one (see the solid and dashed lines in Fig. 4(a)). As indicated by the behavior of the electric bias ΔV in Fig. 4(b), electron transport behavior under both positive and negative thermal biases resembles that of positive thermal bias case that shown in Fig. 3. Meanwhile, the magnitude of the electric bias ΔV of positive thermal bias is enhanced because of the photon-electrical effect. When the microwave field is applied on the left hotter lead, the photon-induced peaks in the bias voltage are smoothed off due to thermal effects. The above trends of the heat current and ΔV hold

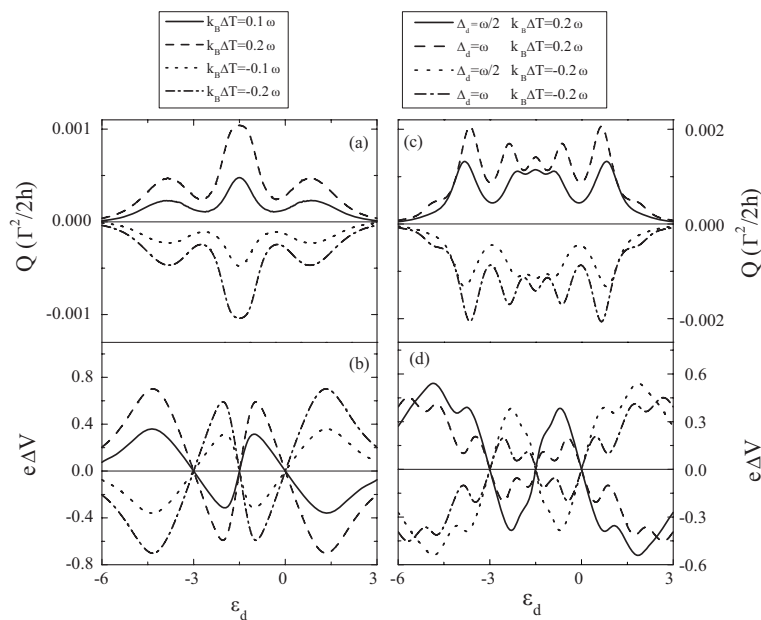


Figure 3. (a) Heat current Q and (b) bias voltage ΔV induced by different thermal bias ΔT as functions of dot level ϵ_d in the absence of microwave field. The temperatures of the left and right leads are $T_L = T + \Delta T/2$ and $T_R = T - \Delta T/2$ with $k_B T = 0.25\omega$. Other parameters are as in Fig. 1. (c-d) same as (a-b) for different thermal bias and in the presence of various microwave strength Δ_d (detailed in the legend), keeping $\Delta_L = \Delta_R = 0$. Both the heat current and the induced voltage exhibit a decrease of their maximum values, and the appearance of additional microwave-induced peaks. The heat always flows from the hot to the cold lead.

true even for zero thermal bias case.

We now qualitatively discuss the impact of phonon on the figure of merit and the heat current. At low temperature regime, we can add to the thermal conductance κ in Eq. (12) a phonon contribution which is $\kappa_{ph} = 3\pi^2 k_B^2 T/h$ [16]. Then the magnitude of ZT will be reduced correspondingly. But the trend of ZT can be unchanged [19]. In the non-linear case, phonon peaks in the heat current may also emerge, which should be an interesting topic. Nevertheless, recent studies indicated that the heat current delivered by phonons can be blocked by particular device design [19], and moreover, κ_{ph} can be small depending on the phonon spectrum [41,42].

4. Discussion and summary

The result presented in the last section is rather surprising: although energy (via the microwave field) is pumped into the bright lead, still heat flows from the dark to the bright lead. The explanation for this effect we point out that the microwave field shifts the spectral weight of the electrons in multiples of the photon frequency, thus effectively reduces the density of states (DOS) in some places and increases it in others. In this case, the effective reduction of the DOS is most pronounced near the particle-hole symmetry point, and the weight is shifted below it. The result is electrons, which are flowing from

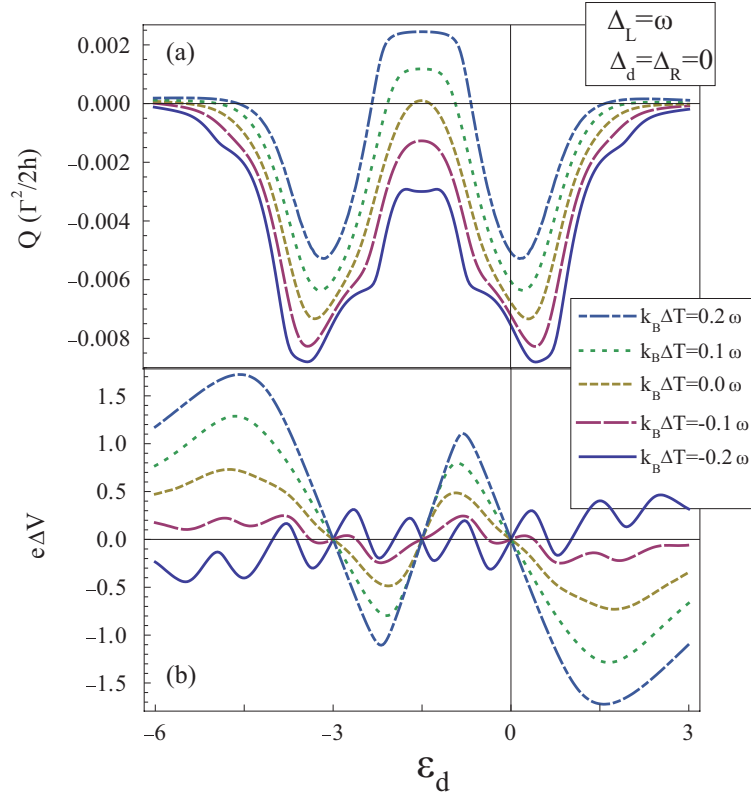


Figure 4. Heat current Q (a) and bias voltage ΔV (b) as functions of dot level ε_d for different thermal bias $k_B \Delta T = -0.2\omega, -0.1\omega, 0, 0.1\omega, 0.2\omega$. A microwave field $\Delta_L = \omega$ is applied only to the left lead. Other parameters are as in Fig. 3. Due to the asymmetry in the microwave field, heat current flows from the dark to the bright lead almost regardless of the temperature gradient, except at the vicinity of particle-hole symmetric point $\varepsilon_d = -U/2$.

the bright to the dark lead, carry *negative* energies, because they are placed below the Fermi energy.

To understand this unique situation it is useful to turn to the analogy with the non-interacting dot where $U = 0$. In that case, the dot is a simple resonant level, and consequently $\text{Im}\langle A_{\beta\sigma}(\varepsilon, t) \rangle$ is simplified,

$$\text{Im}\langle A_{\beta\sigma}(\varepsilon, t) \rangle = \sum_k J_k^2\left(\frac{\Delta_\beta}{\omega}\right) \frac{\Gamma}{(\varepsilon - \varepsilon_d - k\omega)^2 + \Gamma^2}. \quad (13)$$

Substituting it back to Eq. (3) one obtains for the heat current

$$Q = \frac{2}{h} \sum_k \int \varepsilon d\varepsilon \frac{\Gamma}{(\varepsilon - \varepsilon_d - k\omega)^2 + \Gamma^2} [f_L(\varepsilon) J_k^2(\Delta_L/\omega) - f_R(\varepsilon) J_k^2(0)]. \quad (14)$$

The Bessel functions $J_k(x)$ are decaying functions of k for $x \leq 1.434$. Since the Fermi functions decays above the Fermi level, the main contributions to the integral above are $k = 0$ and $k = -1$, resulting in

$$\begin{aligned}
 Q &\approx \frac{2}{h} \int \varepsilon d\varepsilon \frac{\Gamma}{(\varepsilon - \varepsilon_d)^2 + \Gamma^2} [f_L(\varepsilon) J_0^2(\Delta_L/\omega) - f_R(\varepsilon)] \\
 &\quad + \frac{2}{h} \int \varepsilon d\varepsilon \frac{\Gamma}{(\varepsilon - \varepsilon_d + \omega)^2 + \Gamma^2} f_L(\varepsilon) J_1^2(\Delta_L/\omega) \\
 &= \frac{2}{h} \int \varepsilon I(\varepsilon) d\varepsilon.
 \end{aligned} \tag{15}$$

In the absence of the microwave field, the transmission is centered around ε_d and has a single peak, but additional conduction channels open when the microwave field is applied. This can be seen in Fig. 5 where $I(\varepsilon)$ (solid line), which is proportional to the transmission function, and the heat current integrand $\varepsilon I(\varepsilon)$ (dashed line) plotted as functions of the integration variable ε , where we have chosen the dot level $\varepsilon_d = 0$ for clarity. $I(\varepsilon)$ shows an additional peak at negative energies, which induces electron current from the bright to dark leads. The heat current is thus in the opposite direction. Note also that the weight of the negative peak is larger than that of the peak near ε_d , resulting in a net negative heat current.

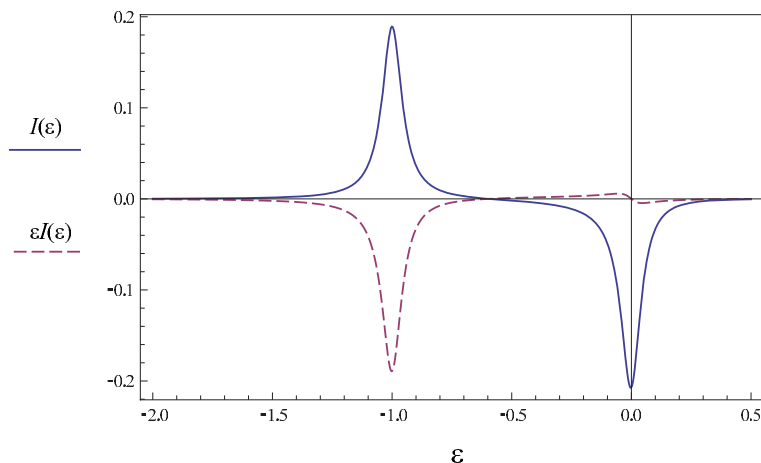


Figure 5. (Color online) $I(\varepsilon)$ (solid line), which is proportional to the transmission function, and the heat current integrand $\varepsilon I(\varepsilon)$ (dashed line) plotted as functions of the integration variable ε for $\varepsilon_d = 0$. An additional peak appears in $I(\varepsilon)$, and when weighted with energy $\varepsilon I(\varepsilon)$ results in negative heat current, i.e. from dark to bright lead.

In summary, microwave-assisted heat transport in a quantum dot is investigated in the framework of nonequilibrium Green's function method. It was found that the figure of merit can be suppressed by a microwave field applied on the dot. In the completely asymmetric case, i.e., the microwave field is applied only on one of the leads, the heat current generally flows from the dark lead to the bright lead, weakly depends on the direction of the thermal bias, and can be reversed only when the dot level is close to the electron-hole symmetry point. The results we have presented here can be verified in experiments similar to those of Ref. [38] in which a temperature difference is applied between the two leads as well as a microwave field and gate voltage. We note that

here we only deal with the fixed microwave frequency case at steady state. One can expect frequency- and time-dependent heat transport will bring about more interesting phenomena, which are beyond the scope of the present paper, and research in that direction is currently underway.

5. Acknowledge

This work was supported by NFS-China (10704011) and LNET (2009R01).

References

- [1] Giazotto F, Heikkilä T T, Luukanen A, Savin A M and Pekola J P 2006 *Rev. Mod. Phys.* 78 217
- [2] Dubi Y and Di Ventra M 2011 *Rev. Mod. Phys.* **83** 131
- [3] Minnich A J, Dresselhaus M S, Ren Z F and Chen G 2009 *Energy Environ. Sci.* 2 466
- [4] Snyder G J and Toberer E S 2008 *Nature Mater.* 7 105
- [5] Kubala B, König J and Pekola J 2008 *Phys. Rev. Lett.* 100, 066801
- [6] Saira O P, Meschke M, Giazotto F, Savin A M, Möttönen M and Pekola J P 2007 *Phys. Rev. Lett.* 99 027203
- [7] Hicks L D and Dresselhaus M S 1993 *Phys. Rev. B* 47 16631
- [8] Lin Y M and Dresselhaus M S 2003 *Phys. Rev. B* 68 075304
- [9] Murphy P, Mukerjee S and Moore J 2008 *Phys. Rev. B* 78 161406(R)
- [10] Kim T S and Hershfield S 2002 *Phys. Rev. Lett.* 88 136601
- [11] Harman T C, Taylor P J, Walsh M P, and LaForge B E 2002 *Science* 297 2229
- [12] Venkatasubramanian R, Siivola E, Colpitts T and OQuinn B 2001 *Nature (London)* 413 597
- [13] Hochbaum A I, Chen R, Delgado R D, Liang W, Garnett E C, Najarian M, Majumdar A and Yang P 2008 *Nature (London)* 451 163
- [14] Boukai A I, Bunimovich Y, Tahir-Kheli J, Kan Y J, Goddard III W A and Heath J R 2008 *Nature (London)* 451 168
- [15] Beenakker C W J and Staring A A M 1992 *Phys. Rev. B* 46 9667
- [16] Dubi Y and Di Ventra M 2009 *Phys. Rev. B* 79 081302(R)
- [17] Zianni X 2010 *Phys. Rev. B* 82 165302
- [18] Kuo D M T and Chang Y C 2010 *Phys. Rev. B* 81 205321
- [19] Świrkowicz R, Wierzbicki M and Barnaś J 2009 *Phys. Rev. B* 80 195409
- [20] Liu J, Sun Q F and Xie X C 2010 *Phys. Rev. B* 81 245323
- [21] Krawiec M and Wysokinski K I 2003 *Phys. Rev. B* 73 075307
- [22] Krawiec M and Wysokinski K I 2007 *Phys. Rev. B* 75 155330
- [23] Scheibner R, Buchmann H, Reuter D, Kiselev M N and Molenkamp L W 2005 *Phys. Rev. Lett.* 95 176602
- [24] Zhou J and Yang R 2010 *Phys. Rev. B* 82 075324
- [25] Liu Y S and Yang X F 2010 *J. Appl. Phys.* 108 023701
- [26] Wierzbicki M and Swirkowicz R 2011 *Phys. Rev. B* 84 075410
- [27] Shakouri A 2006 *Proc. IEEE* 94 1613
- [28] Terraneo M, Peyrard M and Casati G 2002 *Phys. Rev. Lett.* 88 094302
- [29] Wu L A and Segal D 2009 *Phys. Rev. Lett.* 102 095503
- [30] Wang J and Li B 2007 *Phys. Rev. Lett.* 99 177208
- [31] Meschke M, Guichard W and Pekola J P 2006 *Nature (London)* 444 187
- [32] Ojanen T and Jauho A P 2008 *Phys. Rev. Lett.* 100 55902
- [33] Pascal L M A, Courtois H and Hekking F W J 2011 *Phys. Rev. B* 83 125113
- [34] Rey M, Strass M, Kohler S, Hänggi P and Sols F 2007 *Phys. Rev. B* 76 085337

- [35] Ramanayaka A N, Mani R G and Wegscheider W 2011 *Phys. Rev. B* 83 165303
- [36] Lau W T, Shen J T, Veronis G, Fan S H and Braun P V 2008 *Appl. Phys. Lett.* 92 103106
- [37] Crépieux A, Šimkovic F, Cambon B and Michelini F 2011 *Phys. Rev. B* 83 153417
- [38] Kouwenhoven L P, Jauhar S, Orenstein J, McEuen P L, Nagamune Y, Motohisa J and Sakaki H 1994 *Phys. Rev. Lett.* 73 3443
- [39] Jauho A P, Wingreen N S and Meir Y 1994 *Phys. Rev. B* 50 5528
- [40] Sun Q F and Lin T H 1997 *Phys. Rev. B* 56 3591
- [41] Bergfield J P, Solis M A and Stafford C A 2010 *ACS Nano* 4 5314
- [42] Tsaousidou M and Triberis G P 2010 *J. Phys.: Condens. Matter* 22 355304